Title

Soluble epoxide hydrolase inhibitor can protect the femoral head against tobacco smoke exposure-induced osteonecrosis in spontaneously hypertensive rats

Authors

Xu, Jingyi
Qiu, Xing
Yu, Gary
et al.

Publication Date

2022

DOI

10.1016/j.tox.2021.153045

Peer reviewed

HHS Public Access

Author manuscript

Toxicology. Author manuscript; available in PMC 2023 January 15.

Published in final edited form as:

Toxicology. 2022 January 15; 465: 153045. doi:10.1016/j.tox.2021.153045.

Soluble epoxide hydrolase inhibitor can protect the femoral head against tobacco smoke exposure-induced osteonecrosis in spontaneously hypertensive rats

Jingyi Xu[1,*], **Xing Qiu**[1,*], **Gary Yu**[2], **Maria Ly**[2], **Jun Yang**[3], **Rona M Silva**[4], **Xun Zhang**[5], **Mang Yu**[6], **Yinong Wang**[7], **Bruce Hammock**[3], **Kent E. Pinkerton**[4], **Dewei Zhao**[1]

[1]Affiliated Zhongshan Hospital of Dalian University, Dalian, China

[2]Medical Scientist Training Program, University of Pittsburgh, Pittsburgh, PA, USA

[3]Department of Entomology and Nematology, University of California, Davis, CA, USA

[4]Center for Health and the Environment, University of California, Davis, CA, USA

[5]Neuroendocrine Research Laboratory, Harvard University, Cambridge, MA, USA

[6]Department of Pediatrics, Stanford University School of Medicine, Stanford, CA, USA

[7]School of Materials Science and Engineering, Dalian University of Technology, Dalian, China

Abstract

Exposure to tobacco smoke (TS) has been considered a risk factor for osteonecrosis of the femoral head (ONFH). Soluble epoxide hydrolase inhibitors (sEHIs) have been found to reduce inflammation and oxidative stress in a variety of pathologies. This study was designed to assess the effect of sEHI on the development of ONFH phenotypes induced by TS exposure in spontaneously hypertensive (SH) rats. SH and normotensive Wistar Kyoto (WKY) rats were exposed to filtered air (FA) or TS (80 mg/m3 particulate concentration) 6 h/day, 3 days/week for 8 weeks. During this period, sEHI was delivered through drinking water at a concentration of 6 mg/L. Histology, immunohistochemistry, and micro-CT morphometry were performed for phenotypic evaluation. As results, TS exposure induced significant increases in adipocyte area, bone specific surface (BS/BV), and trabecular separation (Tb.SP), as well as significant decreases in bone mineral density (BMD), percent trabecular area (Tb.Ar), HIF-1a expression, bone volume

Correspondence addressed to: Dewei Zhao, M.D., Ph.D., Affiliated Zhongshan Hospital of Dalian University, 6 Jie Fang Street, Dalian, China, 116001, zhaodewei2016@163.com, Phone: +86 13390503299.

*Contribute equally as first author

CRediT authorship contribution statement

Jingyi Xu: Conceptualization, methodology, formal analysis, investigation, data interpretation, writing – original draft. **Xing Qiu**: Investigation, methodology, formal analysis, data interpretation. **Gary Yu**: Formal analysis, data interpretation, and writing – original draft. **Maria Ly**: formal analysis, data interpretation, and writing – original draft. **Kun Wang**: Methodology, formal analysis, data interpretation. **Zhou Liang**: Methodology, formal analysis, and data interpretation. **Jun Yang**: methodology, investigation, formal analysis, and resources. **Rona M. Silva**: investigation, methodology, formal analysis, and data interpretation. **Xun Zhang:** Resources, conceptualization, data interpretation. **Mang Yu**: Conceptualization, methodology, data interpretation, and writing – original draft. **Yinong Wang**: Conceptualization, methodology, data interpretation. **Bruce Hammock**: Resources, conceptualization, methodology, and data interpretation. **Kent E. Pinkerton**: conceptualization, methodology, data interpretation, and supervision. **Dewei Zhao**: Conceptualization, methodology, resources, supervision, data interpretation, and funding acquisition.

Conflict of interest

The authors declare that they have no conflict of interest.

fraction (BV/TV), trabecular numbers (Tb.N), and trabecular thickness (Tb.Th) in both SH and WKY rats. However, the protective effects of sEHI were mainly observed in TS-exposed SH rats, specifically in the density of osteocytes, BMD, Tb.Ar, HIF-1a expression, BV/TV, BS/BV, Tb.N, and Tb.SP. Our study confirms that TS exposure can induce ONFH especially in SH rats, and suggests that sEHI therapy may protect against TS exposure-induced osteonecrotic changes in the femoral head.

Keywords

Tobacco smoke; Osteonecrosis the femoral head; Spontaneously hypertensive rats; Soluble epoxide hydrolase inhibitors

1. Introduction

Osteonecrosis of the femoral head (ONFH) remains a significant clinical challenge (Mont et al., 2006). Epidemiological data showed an incidence of ONFH in the United States between 300 to 600 thousand cases in the early 2000s, with an annual onset of about 10 to 20 thousand new cases (Aldridge and Urbaniak, 2004; Choi et al., 2015; Lieberman et al., 2003). Recently, tobacco smoke (TS) has been recognized as a key independent risk factor for bone loss and increased fracture risk (Kanis et al., 2005; Krall and Dawson-Hughes, 1999; Patel et al., 2013). Specifically, a national survey of 30,030 individuals in China found that there was significantly elevated risk for non-traumatic ONFH associated with TS exposure (D. W. Zhao et al., 2015). This relationship was also demonstrated in a previous study of spontaneously hypertensive (SH) rats, an established model of ONFH when exposed to TS (Xu et al., 2018).

Smoking and hypertension are both risk factors for endothelial dysfunction and cardiovascular and cerebrovascular events (Naito et al., 1993). Reports suggest that endothelial dysfunction, cardiovascular and cerebrovascular events are closely related to femoral head necrosis (Sung et al., 2018). As the SH rat model demonstrates a wide variety of phenotypic similarities to human disease including hormonal imbalances, oxidative stress, inflammation, and hypercoagulation (Karanovic et al., 2021; Kozlowska et al., 2019; F. F. Wang et al., 2021), investigation of novel therapeutic interventions in the SH rat TS exposure model has direct applicability toward future translation and improving our understanding of the pathophysiologic mechanisms between hypertension, TS exposure, and ONFH. Komiyama et al. (Komiyama et al., 2006) found that 5 to 20 weeks of age was a critical period for the exhibition of ossification disturbance, incomplete ossification, and osteonecrosis in the SH rats, and vascular endothelial growth factor (VEGF) played an important role in such processes. So, we selected 12 weeks of rats exposed to smoking until 20 weeks of age to observe the changes of the femoral head.

Soluble epoxide hydrolase inhibitors (sEHI) are antihypertensive agents which prevent the degradation of epoxyeicosatrienoic acids and have been shown to have benefits in numerous cardiovascular diseases including hypertension, renal disease, and stroke (Guedes et al., 2018; Imig and Hammock, 2009; Imig et al., 2005; Khan et al., 2013; Lee et al., 2014; Morisseau and Hammock, 2013; L. Wang et al., 2012; W. Zhang et al., 2007; X. Zhao et al.,

2004). In addition, a previous study showed that sEHI treatment was anti-inflammatory after acute tobacco smoke exposure (Smith et al., 2005). Given that there have been numerous hypotheses regarding the role of vascular disease and endothelial dysfunction in ONFH, as well as the mainstay role of vascular disease in the SH rat model of osteonecrosis (Chiamvimonvat et al., 2007; Cui et al., 2021; Kerachian et al., 2006; Shibahara et al., 2000), we hypothesize that sEHI treatment may confer therapeutic benefits in ONFH worsened from tobacco smoke exposure.

Therefore, in the present study, SH and normotensive Wister-Kyoto (WKY) rats received tobacco smoke exposure with and without sEHI treatment with filtered air controls. Development and extent of ONFH were characterized with histopathologic analyses and microCT assessment, as well as immunohistochemistry for key vascular factors mediating angiogenesis and intraosseous hypoxic stress responses.

2. Methods

2.1. Rats

Twelve-week-old male normotensive WKY and SH rats (n=6 per group; Charles River Laboratories, Portage, MI) were purchased and housed in polycarbonate cages（two rats per cage） with bedding(Harlan Company, Indianapolis, Indiana) under a 12-hour light-dark cycle with continuous access to food （Lab Diet 5001 Rodent Diet, Newco Company, Rancho Cucamonga, California） and water. They were allowed to acclimate for one-week prior to the onset of experimental exposures. Animals were handled in accordance with standards established by the US Animal Welfare Acts as set forth in the National Institutes of Health guidelines and by the University of California, Davis, Animal Care and Use Committee. Rats were euthanized by interperitoneal injection with Pentobarbital (100mg/kg).

2.2. Treatment groups:

Both groups of WHY and SH rats were randomized to filtered air (FA), mixed side stream tobacco smoke (TS), or TS with sEHI treatments. TS exposure was maintained at a particulate concentration of 90 mg total suspended particulates (TSP) per cubic meter for 6 hours each day, 3 days per week for 8 weeks using the TE-10 smoke exposure system combusting 3R4F research cigarettes (Nicotine=0.73mg/cigarette, Tar = 9.4mg / cigarette, Source: University of Kentucky) with a 35 mL puff volume over 2 seconds. Measurements of tobacco smoke constituents were taken at regular intervals of 30 minutes for carbon monoxide, 2 hours for total suspended particulates, and once daily for nicotine(Table 1). sEHI 1-trifluoromethoxyphenyl-3-(1-propionylpiperidin-4-yl) urea (TPPU) was delivered through the drinking water dissolved in a polyethylene glycol-400 (PEG) vehicle at a concentration of 6 mg/L (water intake is about 35ml/d, equivalent to 1mg/kg TPPU/kg body weight) (Zhang et al., 2020) Groups not receiving sEHI received only the vehicle (0.2% PEG-400) in drinking water.

2.3. Micro-CT bone structural analysis

The left femur head structure of each animal was analyzed using micro-CT (Siemens, Inveon MM system, USA). Three-dimensional bone structure parameters and image slices were analyzed and reconstructed (Inveon Acquisition Workplace V1.5, Research Workplace V4.1). These included total bone mineral density (BMD), cortical thickness (Ct.Th), bone volume (BV) per unit total volume (BV/TV), trabecular separation (Tb.Sp), and trabecular thickness (Tb.Th).

2.4. Histopathologic assessment of femoral head

Femoral head samples were decalcified for 20 days in 10% tetrasodium-EDTA and 4% phosphate buffered formalin solution. The femoral heads were then paraffin-embedded and sectioned at a 5-micron thickness and H&E stained (American Tech Master Scientific Inc., Lodi, CA). Stained bone sections were used for quantification of trabecular area, osteocyte number, number of empty lacunae, and adipocyte area. Five randomly-selected non-necrotic sights were used for each section, with blind counts performed by JX and KW. Trabecular bone staining was analyzed for area using Image-Pro Plus software (Image-Pro Plus version 6.0, Media Cybernetics). Epiphyseal cartilage ossification and osteonecrosis were also classified according to a 4-stage system (Table 2). Staging of epiphysis cartilage ossification is based upon histology degree of epiphysis in both SHR and WKY. Femoral heads were classified to four stages: stage 0 (indicating ossification less than 1/2 of the femoral head), stage 1 (indicating ossification of 1/4 to 1/2 of the femoral head), stage 3 (indicating ossification of 1/2 to 3/4 of the femoral head), and stage 3 (indicating ossification of more than 3/4 of the femoral head). Stage of osteonecrosis is determined based upon histology degree of epiphysis in both SHR and WKY: stage 0 (osteonecrosis area less than ¼), stage 1 (osteonecrosis area between ¼ to ½), stage 2 (osteonecrosis area between ½ to ¾), and stage 3 (osteonecrosis area more than ¾).

2.5. Immunohistochemistry

Immunohistochemistry (IHC) staining to determine tissue expression of vascular endothelial growth factor (VEGF) and hypoxia inducible factor-1α (HIF-1α) was performed to assess changes of angiogenesis and hypoxia stress in the femoral heads, respectively. Briefly, the tissue sections were subjected to 3% hydrogen peroxidase for 10 minutes to deactivate the endogenous peroxidase activity and rinsed in PBS. After being blocked with 10% goat normal antiserum for 30 min at room temperature, tissue sections were incubated with primary antibodies (rabbit anti-rat VEGF or HIF-1a polyclonal antibodies, with rabbit polyclonal IgG as isotype controls, Abcam, Waltham, MA, USA) overnight at 4°C, followed by incubation with biotinylated secondary antibodies (goat anti-rabbit) for 30 minutes. Immunoreactivity was visualized using diaminobenzidine (DAB) as the substrate. All sections were counterstained with hematoxylin. All slides were coded and counted without knowledge of the treatment groups. For each slide, 5 non-necrotic sights were randomly selected for intensity scoring and proportion scoring, respectively. The average intensity of cellular staining was visually scored 0 (none, for negatively stained cells), 1 (weak), 2 (moderate), and 3 (strong), respectively, while the proportion of staining was scored 0

(positive area <5%), 1 (positive area 5 – 25%), 2 (positive area 26 – 50%), 3 (positive area 51 – 75%), and 4 (positive area >75%), respectively.

2.6. Statistical analysis

All quantitative parameters were analyzed using 2-way analysis of variance (ANOVA) with Sidak's multiple comparisons post-hoc test with animal group (WKY and SH) and respiratory exposure as main effects. Statistical significance was considered at $P < 0.05$. All results are presented as mean with error bars indicating standard deviation.

3. Results

3.1. General observation

All the smoking rats had sparse hairiness, and drinking less water compare to un-smoke rats, obviously at one day after smoke. Body weight of TS exposed SHR gain not obviously with the extension of time, but un-exposed SHR weight increased significantly with time. The WKY rats increased body weight in varying degrees with the extension of time, and unexposed WKY rats was more pronounced than TS exposed. The application of SEHI did not improve the weight of rats.

The WKY FA rats all had more than half ossification of the femoral head. Qualitatively, trabecular bone of these animals was observed to have uniform distribution, thickness, and orderly arrangement. This is contrasted with the SH TS group, in which no animals had complete ossification, and two thirds of animals had less than half ossification of the femoral head.

Qualitatively, the trabecular bone was observed to be thinner with more disorganized arrangement in these animals. Remaining distributions of both ossification and osteonecrosis among all animal groups are shown in Tables 2 and 3. Although the TS exposure group showed greater rates of increased osteonecrosis than the FA group for each rat type respectively, the SH TS group demonstrated a reduced rate of osteonecrosis with addition of sEHI that was equal to the WKY-FA group.

3.2. Histopathological changes of the femoral head

As shown in the histological images in Figure 1, there were distinct qualitative changes in the appearance of the femoral head when rats of both groups were exposed to TS (Fig. 1, A *vs.* C and B *vs.* D). Specifically, the trabecular bone showed a looser appearance with increased space in the bone marrow cavity, increased porosity, and sparse, thin trabecular organization. The severity of these changes was greater for the SH rats compared to the WKY rats (Fig. 1, C *vs.* D). However, with sEHI treatment as shown in Fig. 1E and 1F, the debilitative changes associated with TS exposure are not observed, and the tissue appears more qualitatively similar to the FA exposure group. However, the SH TS-sEHI group did show some remaining traces of osteonecrosis, indicating that sEHI was not completely protective against TS exposure.

Quantitative measures of histopathological changes included number of empty lacunae, adipocyte area, trabecular area, and osteocyte concentration (Fig. 2). SH TS rats showed

a significantly increased number of empty lacunae compared to FA and TS-sEHI groups (Fig. 2A, $P < 005$, respectively). However, the SH FA and SH TS-sEHI groups demonstrated no significant differences in number of empty lacunae (Fig. 2A). There was significantly increased adipocyte area with TS exposure in SH rats while the increase in WKY rats was not statistically significant (Fig. 2B). SH rats showed significant improvements in both trabecular area as well as osteocyte concentration with sEHI treatment after TS exposure (Fig. 2, C and D), while WKY rats did not demonstrate an increase in trabecular area with sEHI treatment after statistically significant loss of trabecular area after TS exposure (Fig. 2C). Finally, WKY rats did not share the decrease in osteocyte concentration after TS exposure seen in SH rats (Fig. 2D).

3.3. Immunohistochemistry of femoral heads

Immunohistochemistry images and results of immunohistochemistry analysis of HIF-1a and VEGF expression are shown in Figures 3. SH rats exposed to TS showed significantly decreased levels of both HIF-1a and VEGF expression compared to WKY rats exposed to TS (Fig. 3, C and D). However, sEHI treatment resulted in significantly increased levels of HIF-1a in SH rats only to levels similar to SH rats exposed to FA (Fig. 3C). There was a greater quantitative decrease in VEGF for SH rats trending toward statistical significance compared to FA exposure not seen in WKY rats, in which VEGF expression remained similar between TS and FA exposure (Fig. 3D).

3.4. Microstructure analysis of femoral heads

Representative micro-CT images of rat femoral heads are shown in Figure 4. Qualitative decreases in ossification were observed with TS exposure for both animal groups (Fig. 4, A *vs.* C and B *vs.* D). Improvements in ossification with sEHI treatment after TS exposure were seen in SH animals but were absent in WKY animals (Fig. 4, E *vs.* C and F *vs.* D).

Quantitative parameters of ossification and microstructural organization showed similar trends of improvement for SH animals receiving sEHI treatment after TS exposure (Fig. 5). Bone mineral density, bone volume fraction, and number of trabeculae all showed statistically significant increases with sEHI treatment after TS exposure in SH rats to levels statistically similar to the SH FA exposure group (Fig. 5, A to C). Bone mineral density and volume fraction remained depressed in WKY rats after TS exposure regardless of sEHI treatment (Fig. 5A). In addition, SH rats demonstrated statistically significant changes in trabecular thickness and bone surface-to-volume fraction after TS exposure not shared by the WKY group (Fig. 5, D and E). Again, trabecular thickness and bone surface-to-volume fraction returned to levels similar to the FA controls for SH rats after sEHI treatment (Fig. 5, D and E). The trabecular separation of SH rats was significantly higher than that of WKY rats for FA and TS exposure groups. However, there was no significant difference in trabecular separation for the groups after sEHI treatment following TS exposure (Fig. 5F).

4. Discussion

In a previous study, we showed that TS exposure led to significant increases in ossification delay, bone microstructural damage, and histopathological changes associated with ONFH

in SH rats (Xu et al., 2018). These findings were consistent with results of clinical investigations on the relationship between TS and ONFH, including multiple case-control studies showing an increased risk of ONFH in tobacco smokers (Wen et al., 2017). To our knowledge, the present study is the first application of sEHI for the treatment of TS-induced ONFH in SH rats. Our results have shown that sEHI is protective against the debilitative microstructural and histopathological changes in the femoral head associated with TS exposure. This protective effect resulted in the return of microstructural and histopathological measures of the TS-sEHI group to levels seen in the SH FA control group. More specifically, the measures evaluated represent key pathologic indicators of early ONFH or ONFH progression, including hyperplastic adipocytes, empty lacunae, mineralization, and trabecular microstructural organization. These results were primarily seen in the previously validated SH rat model of ONFH (Xu et al., 2018); while the WKY control group showed similar changes after TS exposure to a lesser extent, the sEHI treatment did not show significant efficacy, suggesting that the therapeutic mechanism of sEHI may target a pathologic characteristic of SH rats.

Possible mechanistic explanations for the therapeutic efficacy for sEHI against ONFH likely involve the underlying vascular endothelial pathophysiology related to inflammation, oxidative stress, and the hypoxic response (Chiamvimonvat et al., 2007; Imig and Hammock, 2009; Kerachian et al., 2006). This is supported by the increase in HIF-1a expression after sEHI treatment and the similar but not statistically significant increase in VEGF expression. The role of VEGF in promoting angiogenesis and osteogenesis has be well documented (Dreyer et al., 2020; Hu and Olsen, 2016; Li et al., 2016). Beyond upregulating VEGF expression (in hypoxic tissues) and inducing mesenchymal stem cell differentiation to osteoblast and osteocyte, HIF-1a can enhance the formation of type H blood vessels in the metaphyseal region and sub-periosteum during osteogenesis (Peng et al., 2020; Yellowley and Genetos, 2019; J. Zhang et al., 2020). Previous models of TS-induced limb ischemia and lung injury have demonstrated that decreased expression of HIF-1a and VEGF are mechanistic mediators of TS-induced inflammation and loss of angiogenesis (Basic et al., 2012; Daijo et al., 2016; Michaud et al., 2003; Pouya and Kerachian, 2015). Inflammation and reduced angiogenesis are also considered key factors in the pathogenesis of ONFH in current vascular hypotheses (Cui et al., 2021; Kerachian et al., 2006; Pouya and Kerachian, 2015). In addition, other previous investigations of therapeutic applications of sEHI in the context of vascular disease have also emphasized its anti-inflammation and vasodilatory effects(Imig et al., 2009; Imig et al., 2012; Khan et al., 2013), which may certainly also share applicability to ONFH in which maintaining blood supply to the femoral head is a key aspect of preventing disease progression.

Hyperplastic adipocytes and increased empty lacuna both are early pathological indicators of ONFH (Bermeo et al., 2014; Vaughan et al., 2015). Significantly increased number of empty lacuna and adipocyte area exhibited in the TS SH rats indicated that TS exposure inhibited osteogenesis, leading to the pathological change of ONFH. Given that the bone marrow stem cells (BMSCs) are capable of differentiation towards adipocytes as well as osteoblasts (Gimble, 1990; Gimble et al., 2006), significantly increased intramedullary adipocytes, as observed in the TS SHR group, may indicate diversion of BMSC differentiation from osteoblasts to adipocytes, which contributes to bone loss. In addition, TS-inhibited VEGF

expression may theoretically slow the development of the preliminary ossification center and the subsequent formation of mature bone tissue (Cohen, 2006). Thus, our data confirm that sEHI treatment is associated with significantly increased trabecular area and osteocyte concentration, which significantly contributes to bone formation in the femoral head.

Recently, micro-CT has been considered the gold standard for assessing bone morphology and microarchitecture in small animal models, which contributes to the reconstruction of a 3D representation of the bone to show the spatial distribution of bone mineral density (Bouxsein et al., 2010). Micro-CT-derived 2D and 3D morphologic measurements highly complement those from 2D histomorphometry (Alexander et al., 2001; Barbier et al., 1999; Kapadia et al., 1998). For example, femoral heads from WKY versus SH rats subjected to FA exhibit similar 2D histomorphometric features, however, micro-CT-aided measurements clearly demonstrated the changes in trabecular bone microarchitecture linked to bone loss in the FA SH rats. Our data demonstrate that sEHI treatment can maintain BMD, bone volume fraction, as well as trabecular number, thickness, and separation following TS exposure, demonstrating the protective effect against TS-induced bone loss. These micro-CT-derived morphological characters are consistent with those generated from histomorphometry showing that sEHI treatment maintains the number of empty lacunae and percent trabecular area, as well as the concentration of osteocytes in the tissue in SH rats subjected to TS exposure.

Our data further confirms that the SH rat provides a useful model for the study of TS exposure induced ONFH. It has been well documented that spontaneously hypertensive rats exhibit spontaneously developed phenotypes of ONFH, which may make them more susceptible to steroid usage and exposure to TS (Murata et al., 2007; Xu et al., 2018). In the present study, femoral heads from WKY versus SH rats subjected to FA exhibit similar 2D histomorphometric features, however, micro-CT-aided measurements clearly demonstrated the changes in trabecular bone microarchitecture linked to bone loss in the FA SH rats. Such changes in the microarchitecture of the femoral head in SH rats may make the femoral head more susceptible to TS induced osteonecrosis. Accordingly, SH rats also exhibited higher responsiveness versus WKY rats to sEHI therapy against TS-induced osteonecrotic changes in the femoral heads. The underlying mechanisms remain to be investigated.

Taken together, this study proposes that exposure to TS is a significant risk factor of ONFH, especially in the individuals with hypertension, and sEHI treatment is protective against osteonecrotic changes induced by TS exposure.

Acknowledgments

The authors would like to thank Dale Uyeminami for technical expertise with animal care and tobacco smoke exposure, as well as Imelda Espiritu for histology services.

Role of the funding source

The project was supported by the Doctoral Program Foundation of Dalian University (No.1201012). Partial support was also provided by NIEHS/R01 ES002710 and Superfund P42 ES004699. The funders had no role in study design, data collection and analysis, decision to publish, or preparation of the manuscript.

References

Aldridge JM 3rd, Urbaniak JR, 2004. Avascular necrosis of the femoral head: etiology, pathophysiology, classification, and current treatment guidelines. Am J Orthop (Belle Mead NJ) 33, 327–332. [PubMed: 15344574]

Alexander JM, Bab I, Fish S, Muller R, Uchiyama T, Gronowicz G, Nahounou M, Zhao Q, White DW, Chorev M, Gazit D, Rosenblatt M, 2001. Human parathyroid hormone 1–34 reverses bone loss in ovariectomized mice. J Bone Miner Res 16, 1665–1673. 10.1359/jbmr.2001.16.9.1665. [PubMed: 11547836]

Barbier A, Martel C, de Vernejoul MC, Tirode F, Nys M, Mocaer G, Morieux C, Murakami H, Lacheretz F, 1999. The visualization and evaluation of bone architecture in the rat using three-dimensional X-ray microcomputed tomography. J Bone Miner Metab 17, 37–44. 10.1007/s007740050061. [PubMed: 10084400]

Basic VT, Tadele E, Elmabsout AA, Yao H, Rahman I, Sirsjo A, Abdel-Halim SM, 2012. Exposure to cigarette smoke induces overexpression of von Hippel-Lindau tumor suppressor in mouse skeletal muscle. Am J Physiol Lung Cell Mol Physiol 303, L519–527. 10.1152/ajplung.00007.2012. [PubMed: 22842216]

Bermeo S, Gunaratnam K, Duque G, 2014. Fat and bone interactions. Curr Osteoporos Rep 12, 235–242. 10.1007/s11914-014-0199-y. [PubMed: 24599601]

Bouxsein ML, Boyd SK, Christiansen BA, Guldberg RE, Jepsen KJ, Muller R, 2010. Guidelines for assessment of bone microstructure in rodents using micro-computed tomography. J Bone Miner Res 25, 1468–1486. 10.1002/jbmr.141. [PubMed: 20533309]

Chiamvimonvat N, Ho CM, Tsai HJ, Hammock BD, 2007. The soluble epoxide hydrolase as a pharmaceutical target for hypertension. J Cardiovasc Pharmacol 50, 225–237. 10.1097/FJC.0b013e3181506445. [PubMed: 17878749]

Choi HR, Steinberg ME, E YC, 2015. Osteonecrosis of the femoral head: diagnosis and classification systems. Curr Rev Musculoskelet Med 8, 210–220. 10.1007/s12178-015-9278-7. [PubMed: 26088795]

Cohen MM Jr., 2006. The new bone biology: pathologic, molecular, and clinical correlates. Am J Med Genet A 140, 2646–2706. 10.1002/ajmg.a.31368. [PubMed: 17103447]

Cui Q, Jo WL, Koo KH, Cheng EY, Drescher W, Goodman SB, Ha YC, Hernigou P, Jones LC, Kim SY, Lee KS, Lee MS, Lee YJ, Mont MA, Sugano N, Taliaferro J, Yamamoto T, Zhao D, 2021. ARCO Consensus on the Pathogenesis of Non-traumatic Osteonecrosis of the Femoral Head. J Korean Med Sci 36, e65. 10.3346/jkms.2021.36.e65. [PubMed: 33724736]

Daijo H, Hoshino Y, Kai S, Suzuki K, Nishi K, Matsuo Y, Harada H, Hirota K, 2016. Cigarette smoke reversibly activates hypoxia-inducible factor 1 in a reactive oxygen species-dependent manner. Sci Rep 6, 34424. 10.1038/srep34424.

Dreyer CH, Kjaergaard K, Ding M, Qin L, 2020. Vascular endothelial growth factor for in vivo bone formation: A systematic review. J Orthop Translat 24, 46–57. 10.1016/j.jot.2020.05.005. [PubMed: 32642428]

Gimble JM, 1990. The function of adipocytes in the bone marrow stroma. New Biol 2, 304–312. [PubMed: 2288904]

Gimble JM, Zvonic S, Floyd ZE, Kassem M, Nuttall ME, 2006. Playing with bone and fat. J Cell Biochem 98, 251–266. 10.1002/jcb.20777. [PubMed: 16479589]

Guedes AGP, Aristizabal F, Sole A, Adedeji A, Brosnan R, Knych H, Yang J, Hwang SH, Morisseau C, Hammock BD, 2018. Pharmacokinetics and antinociceptive effects of the soluble epoxide hydrolase inhibitor t-TUCB in horses with experimentally induced radiocarpal synovitis. J Vet Pharmacol Ther 41, 230–238. 10.1111/jvp.12463. [PubMed: 29067696]

Hu K, Olsen BR, 2016. The roles of vascular endothelial growth factor in bone repair and regeneration. Bone 91, 30–38. 10.1016/j.bone.2016.06.013. [PubMed: 27353702]

Imig JD, Carpenter MA, Shaw S, 2009. The Soluble Epoxide Hydrolase Inhibitor AR9281 Decreases Blood Pressure, Ameliorates Renal Injury and Improves Vascular Function in Hypertension. Pharmaceuticals (Basel) 2, 217–227. 10.3390/ph2030217. [PubMed: 27713235]

Imig JD, Hammock BD, 2009. Soluble epoxide hydrolase as a therapeutic target for cardiovascular diseases. Nat Rev Drug Discov 8, 794–805. 10.1038/nrd2875. [PubMed: 19794443]

Imig JD, Walsh KA, Hye Khan MA, Nagasawa T, Cherian-Shaw M, Shaw SM, Hammock BD, 2012. Soluble epoxide hydrolase inhibition and peroxisome proliferator activated receptor gamma agonist improve vascular function and decrease renal injury in hypertensive obese rats. Exp Biol Med (Maywood) 237, 1402–1412. 10.1258/ebm.2012.012225. [PubMed: 23354399]

Imig JD, Zhao X, Zaharis CZ, Olearczyk JJ, Pollock DM, Newman JW, Kim IH, Watanabe T, Hammock BD, 2005. An orally active epoxide hydrolase inhibitor lowers blood pressure and provides renal protection in salt-sensitive hypertension. Hypertension 46, 975–981. 10.1161/01.HYP.0000176237.74820.75. [PubMed: 16157792]

Kanis JA, Johnell O, Oden A, Johansson H, De Laet C, Eisman JA, Fujiwara S, Kroger H, McCloskey EV, Mellstrom D, Melton LJ, Pols H, Reeve J, Silman A, Tenenhouse A, 2005. Smoking and fracture risk: a meta-analysis. Osteoporos Int 16, 155–162. 10.1007/s00198-004-1640-3. [PubMed: 15175845]

Kapadia RD, Stroup GB, Badger AM, Koller B, Levin JM, Coatney RW, Dodds RA, Liang X, Lark MW, Gowen M, 1998. Applications of micro-CT and MR microscopy to study pre-clinical models of osteoporosis and osteoarthritis. Technol Health Care 6, 361–372. [PubMed: 10100939]

Karanovic D, Mihailovic-Stanojevic N, Miloradovic Z, Ivanov M, Vajic UJ, Grujic-Milanovic J, Markovic-Lipkovski J, Dekanski D, Jovovic D, 2021. Olive leaf extract attenuates adriamycin-induced focal segmental glomerulosclerosis in spontaneously hypertensive rats via suppression of oxidative stress, hyperlipidemia, and fibrosis. Phytother Res 35, 1534–1545. 10.1002/ptr.6920. [PubMed: 33098170]

Kerachian MA, Harvey EJ, Cournoyer D, Chow TY, Seguin C, 2006. Avascular necrosis of the femoral head: vascular hypotheses. Endothelium 13, 237–244. 10.1080/10623320600904211. [PubMed: 16990180]

Khan MA, Liu J, Kumar G, Skapek SX, Falck JR, Imig JD, 2013. Novel orally active epoxyeicosatrienoic acid (EET) analogs attenuate cisplatin nephrotoxicity. FASEB J 27, 2946–2956. 10.1096/fj.12-218040. [PubMed: 23603837]

Komiyama T, Nishida K,Yorimitsu M, Doi H, Miyazawa S, Kitamura A, Yoshida A, Nasu Y, Abe N,Ozaki T, 2006. Decreased levels of insulin-like growth factor-1 and vascular endothelial growth factor relevant to the ossification disturbance in femoral heads spontaneous hypertensive rats.Acta medica Okayama 60, 141–148. 10.18926/AMO/30749. [PubMed: 16838042]

Kozlowska A, Wojtacha P, Rowniak M, Kolenkiewicz M, Tsai ML, 2019. Differences in serum steroid hormones concentrations in Spontaneously Hypertensive Rats (SHR) - an animal model of Attention-Deficit/Hyperactivity Disorder (ADHD). Physiol Res 68, 25–36. 10.33549/physiolres.933907. [PubMed: 30433797]

Krall EA, Dawson-Hughes B, 1999. Smoking increases bone loss and decreases intestinal calcium absorption. J Bone Miner Res 14, 215–220. 10.1359/jbmr.1999.14.2.215. [PubMed: 9933475]

Lee KS, Liu JY, Wagner KM, Pakhomova S, Dong H, Morisseau C, Fu SH, Yang J, Wang P, Ulu A, Mate CA, Nguyen LV, Hwang SH, Edin ML, Mara AA, Wulff H, Newcomer ME, Zeldin DC, Hammock BD, 2014. Optimized inhibitors of soluble epoxide hydrolase improve in vitro target residence time and in vivo efficacy. J Med Chem 57, 7016–7030. 10.1021/jm500694p. [PubMed: 25079952]

Li B, Wang H, Qiu G, Su X, Wu Z, 2016. Synergistic Effects of Vascular Endothelial Growth Factor on Bone Morphogenetic Proteins Induced Bone Formation In Vivo: Influencing Factors and Future Research Directions. Biomed Res Int 2016, 2869572. 10.1155/2016/2869572.

Lieberman JR, Berry DJ, Mont MA, Aaron RK, Callaghan JJ, Rajadhyaksha AD, Urbaniak JR, 2003. Osteonecrosis of the hip: management in the 21st century. Instr Course Lect 52, 337–355. [PubMed: 12690862]

Michaud SE, Menard C, Guy LG, Gennaro G, Rivard A, 2003. Inhibition of hypoxia-induced angiogenesis by cigarette smoke exposure: impairment of the HIF-1alpha/VEGF pathway. FASEB J 17, 1150–1152. 10.1096/fj.02-0172fje. [PubMed: 12709416]

Mont MA, Jones LC, Hungerford DS, 2006. Nontraumatic osteonecrosis of the femoral head: ten years later. J Bone Joint Surg Am 88, 1117–1132. 10.2106/JBJS.E.01041. [PubMed: 16651589]

Morisseau C, Hammock BD, 2013. Impact of soluble epoxide hydrolase and epoxyeicosanoids on human health. Annu Rev Pharmacol Toxicol 53, 37–58. 10.1146/annurev-pharmtox-011112-140244. [PubMed: 23020295]

Murata M, Kumagai K, Miyata N, Osaki M, Shindo H, 2007. Osteonecrosis in stroke-prone spontaneously hypertensive rats: effect of glucocorticoid. J Orthop Sci 12, 289–295. 10.1007/s00776-007-1129-y. [PubMed: 17530382]

Naito S, Ito M, Sekine I, Ito M, Hirano T, Iwasaki K, Niwa T, 1993. Femoral head necrosis and osteopenia in stroke-prone spontaneously hypertensive rats (SHRSPs). Bone 14, 745–53. 10.1016/8756-3282(93)90206-p [PubMed: 8268049]

Patel RA, Wilson RF, Patel PA, Palmer RM, 2013. The effect of smoking on bone healing: A systematic review. Bone Joint Res 2, 102–111. 10.1302/2046-3758.26.2000142. [PubMed: 23836474]

Peng Y, Wu S, Li Y, Crane JL, 2020. Type H blood vessels in bone modeling and remodeling. Theranostics 10, 426–436. 10.7150/thno.34126. [PubMed: 31903130]

Pouya F, Kerachian MA, 2015. Avascular Necrosis of the Femoral Head: Are Any Genes Involved? Arch Bone Jt Surg 3, 149–155. [PubMed: 26213697]

Shibahara M, Nishida K, Asahara H, Yoshikawa T, Mitani S, Kondo Y, Inoue H, 2000. Increased osteocyte apoptosis during the development of femoral head osteonecrosis in spontaneously hypertensive rats. Acta Med Okayama 54, 67–74. 10.18926/AMO/32287. [PubMed: 10806527]

Smith KR, Pinkerton KE, Watanabe T, Pedersen TL, Ma SJ, Hammock BD, 2005. Attenuation of tobacco smoke-induced lung inflammation by treatment with a soluble epoxide hydrolase inhibitor. Proc Natl Acad Sci U S A 102, 2186–2191. 10.1073/pnas.0409591102. [PubMed: 15684051]

Sung P, Yang Y, Chiang HJ, Chiang JY, Chen CJ, Yip HK, Lee MS, 2018. Cardiovascular and Cerebrovascular Events Are Associated With Nontraumatic Osteonecrosis of the Femoral Head. Clin Orthop Relat Res 476, 865–874. 10.1007/s11999.0000000000000161. [PubMed: 29480889]

Vaughan TJ, Voisin M, Niebur GL, McNamara LM, 2015. Multiscale modeling of trabecular bone marrow: understanding the micromechanical environment of mesenchymal stem cells during osteoporosis. J Biomech Eng 137. 10.1115/1.4028986.

Wang FF, Ba J, Yu XJ, Shi XL, Liu JJ, Liu KL, Fu LY, Su Q, Li HB, Kang KB, Yi QY, Wang SQ, Gao HL, Qi J, Li Y, Zhu GQ, Kang YM, 2021. Central Blockade of E-Prostanoid 3 Receptor Ameliorated Hypertension Partially by Attenuating Oxidative Stress and Inflammation in the Hypothalamic Paraventricular Nucleus of Spontaneously Hypertensive Rats. Cardiovasc Toxicol 21, 286–300. 10.1007/s12012-020-09619-w. [PubMed: 33165770]

Wang L, Yang J, Guo L, Uyeminami D, Dong H, Hammock BD, Pinkerton KE, 2012. Use of a soluble epoxide hydrolase inhibitor in smoke-induced chronic obstructive pulmonary disease. Am J Respir Cell Mol Biol 46, 614–622. 10.1165/rcmb.2011-0359OC. [PubMed: 22180869]

Wen Z, Lin Z, Yan W, Zhang J, 2017. Influence of cigarette smoking on osteonecrosis of the femoral head (ONFH): a systematic review and meta-analysis. Hip Int 27, 425–435. 10.5301/hipint.5000516. [PubMed: 28574127]

Xu J, Qiu X, Liang Z, Smiley-Jewell S, Lu F, Yu M, Pinkerton KE, Zhao D, Shi B, 2018. Exposure to tobacco smoke increases bone loss in spontaneously hypertensive rats. Inhal Toxicol 30, 229–238. 10.1080/08958378.2018.1506838. [PubMed: 30257116]

Yellowley CE, Genetos DC, 2019. Hypoxia Signaling in the Skeleton: Implications for Bone Health. Curr Osteoporos Rep 17, 26–35. 10.1007/s11914-019-00500-6. [PubMed: 30725321]

Zhang J, Pan J, Jing W, 2020. Motivating role of type H vessels in bone regeneration. Cell Prolif 53, e12874. 10.1111/cpr.12874. [PubMed: 33448495]

Zhang L, Xu S, Wu X, Muse FM, Chen J, Cao Y, Yan J, Cheng Z, Yi X Han Z, 2020. Protective Effects of the Soluble Epoxide Hydrolase Inhibitor 1-Trifluoromethoxyphenyl-3-(1-Propionylpiperidin-4-yl) Urea in a Rat Model of Permanent Middle Cerebral Artery Occlusion. Frontiers in pharmacology 11,182. 10.3389/fphar.2020.00182. [PubMed: 32184732]

Zhang W, Koerner IP, Noppens R, Grafe M, Tsai HJ, Morisseau C, Luria A, Hammock BD, Falck JR, Alkayed NJ, 2007. Soluble epoxide hydrolase: a novel therapeutic target in stroke. J Cereb Blood Flow Metab 27, 1931–1940. 10.1038/sj.jcbfm.9600494. [PubMed: 17440491]

Zhao DW, Yu M, Hu K, Wang W, Yang L, Wang BJ, Gao XH, Guo YM, Xu YQ, Wei YS, Tian SM, Yang F, Wang N, Huang SB, Xie H, Wei XW, Jiang HS, Zang YQ, Ai J, Chen YL, Lei GH, Li YJ, Tian G, Li ZS, Cao Y, Ma L, 2015. Prevalence of Nontraumatic Osteonecrosis of the Femoral Head and its Associated Risk Factors in the Chinese Population: Results from a Nationally Representative Survey. Chin Med J (Engl) 128, 2843–2850. 10.4103/0366-6999.168017. [PubMed: 26521779]

Zhao X, Yamamoto T, Newman JW, Kim IH, Watanabe T, Hammock BD, Stewart J, Pollock JS, Pollock DM, Imig JD, 2004. Soluble epoxide hydrolase inhibition protects the kidney from hypertension-induced damage. J Am Soc Nephrol 15, 1244–53. https://jasn.asnjournals.org/content/15/5/1244.long. [PubMed: 15100364]

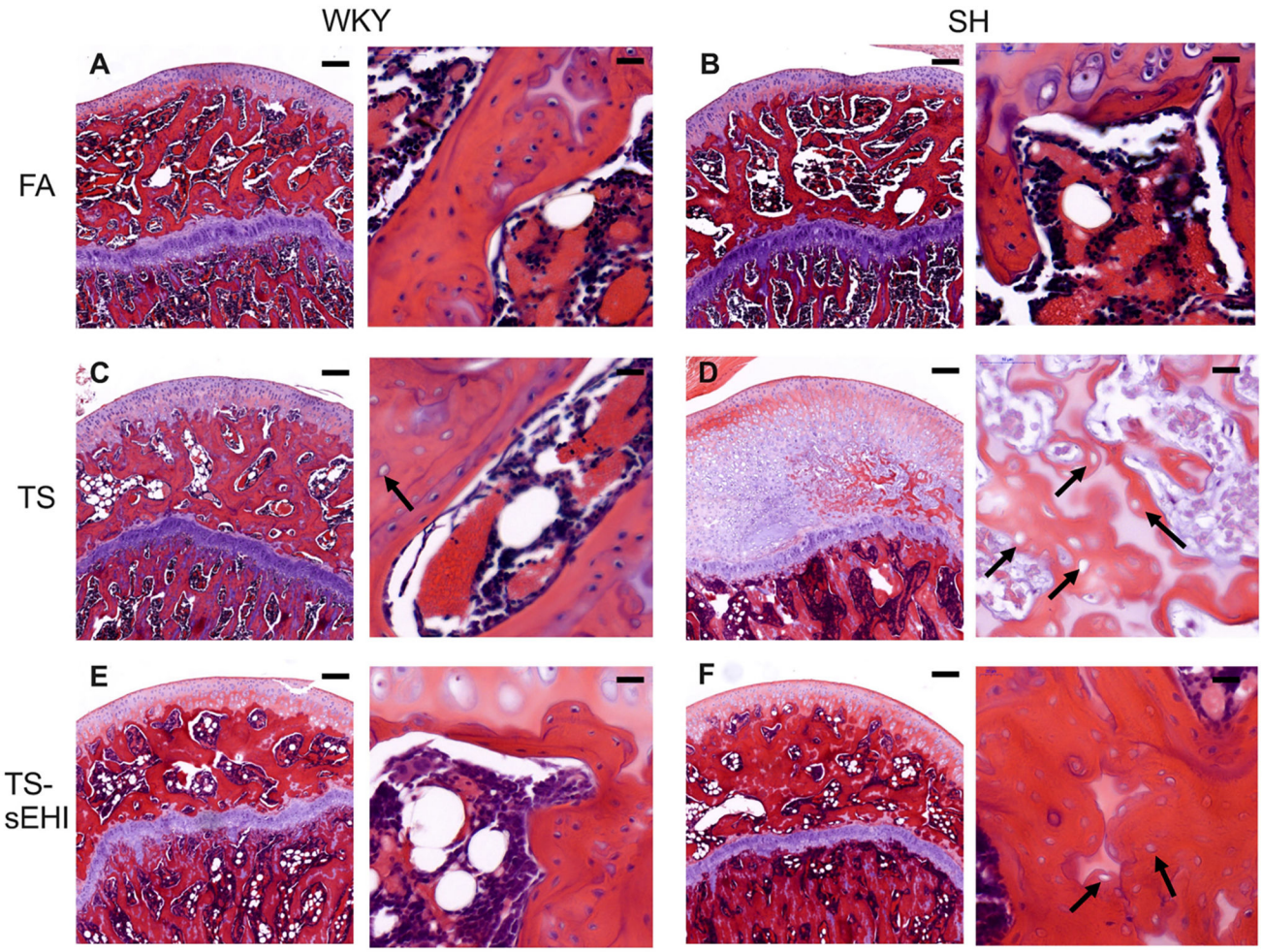

Fig. 1. Influence of TS exposure and sEHI treatment on the histology of the femoral heads.

Representative images of H & E-stained tissue sections from WKY or SH rats subjected to FA, TS, or TS plus sEHI. Arrows indicate empty lacuna. Scale bars = 200 mm, n = 6 per groups. WKY, normotensive Wistar Kyoto rats; SH, spontaneously hypertensive rats; FA, exposure to filtered air; TS, exposure to tobacco smoke; sEHI, treatment with soluble epoxide hydrolase inhibitor.

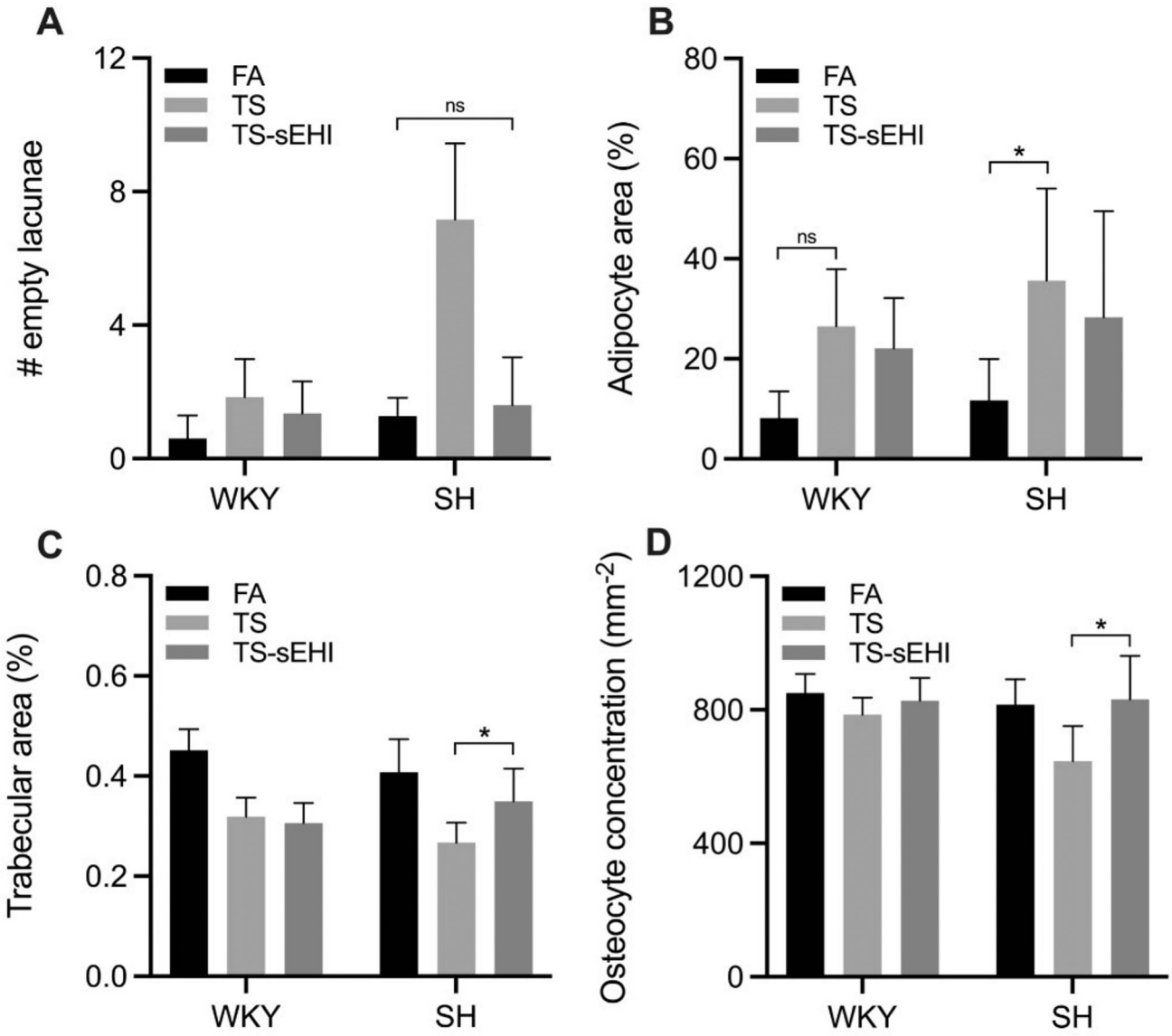

Fig. 2. Influence of TS exposure and sEHI treatment on the cellular components of the femoral heads.

Numbers of empty (**A**), percent adipocyte area (**B**), percent trabecular area (**C**), and osteocyte concentrations (**D**) in the femoral heads from SH and WKY rats subjected to FA (black bars), TS (light gray bars), or TS and sEHI (dark gray bars). * $P < 0.05$ *vs.* the group indicated, ns = not significant, n = 6 per group. WKY, normotensive Wistar Kyoto rats; SH, spontaneously hypertensive rats; FA, exposure to filtered air; TS, exposure to tobacco smoke; sEHI, treatment with soluble epoxide hydrolase inhibitor.

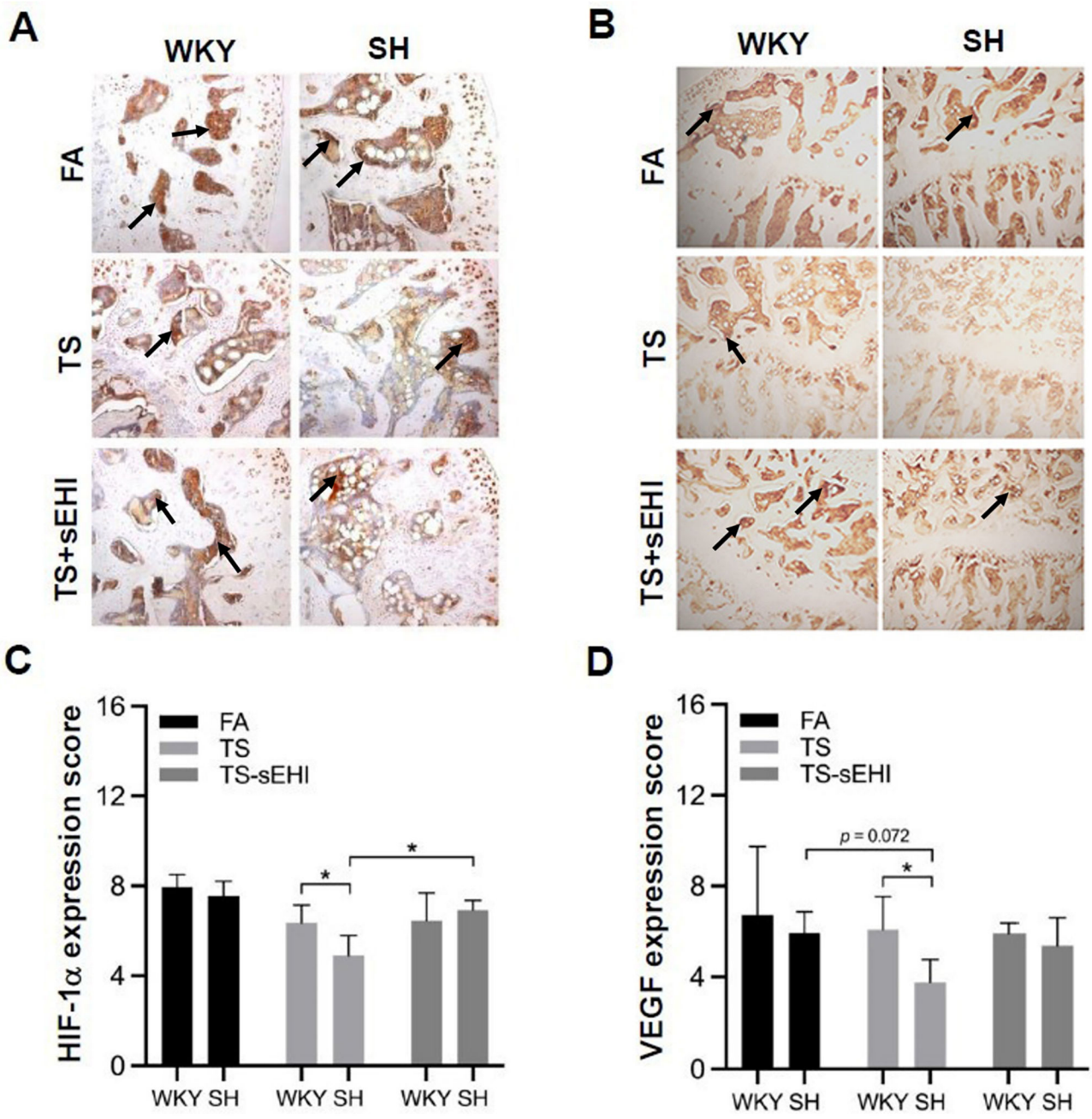

Fig. 3. Influence of TS exposure and sEHI treatment on the expression of HIF-1a and VEGF.

Representative immunohistochemistry images of HIF-1a (**A**) and VEGF (**B**) of the femoral heads from WKY or SH rats subjected to FA, TS, or TS plus sEHI. Arrows indicate typical immunoreactive cells in intramedullary vessels. The intensity of immunostaining was measured to score the expression of HIF-1a (**C**) and VEGF (**D**) of each group. * $P < 0.05$ *vs.* the group indicated, n = 6 per group. WKY, normotensive Wistar Kyoto rats; SH, spontaneously hypertensive rats; FA, exposure to filtered air; TS, exposure to tobacco smoke; sEHI, treatment with soluble epoxide hydrolase inhibitor. Corresponding images of isotypic control staining not shown.

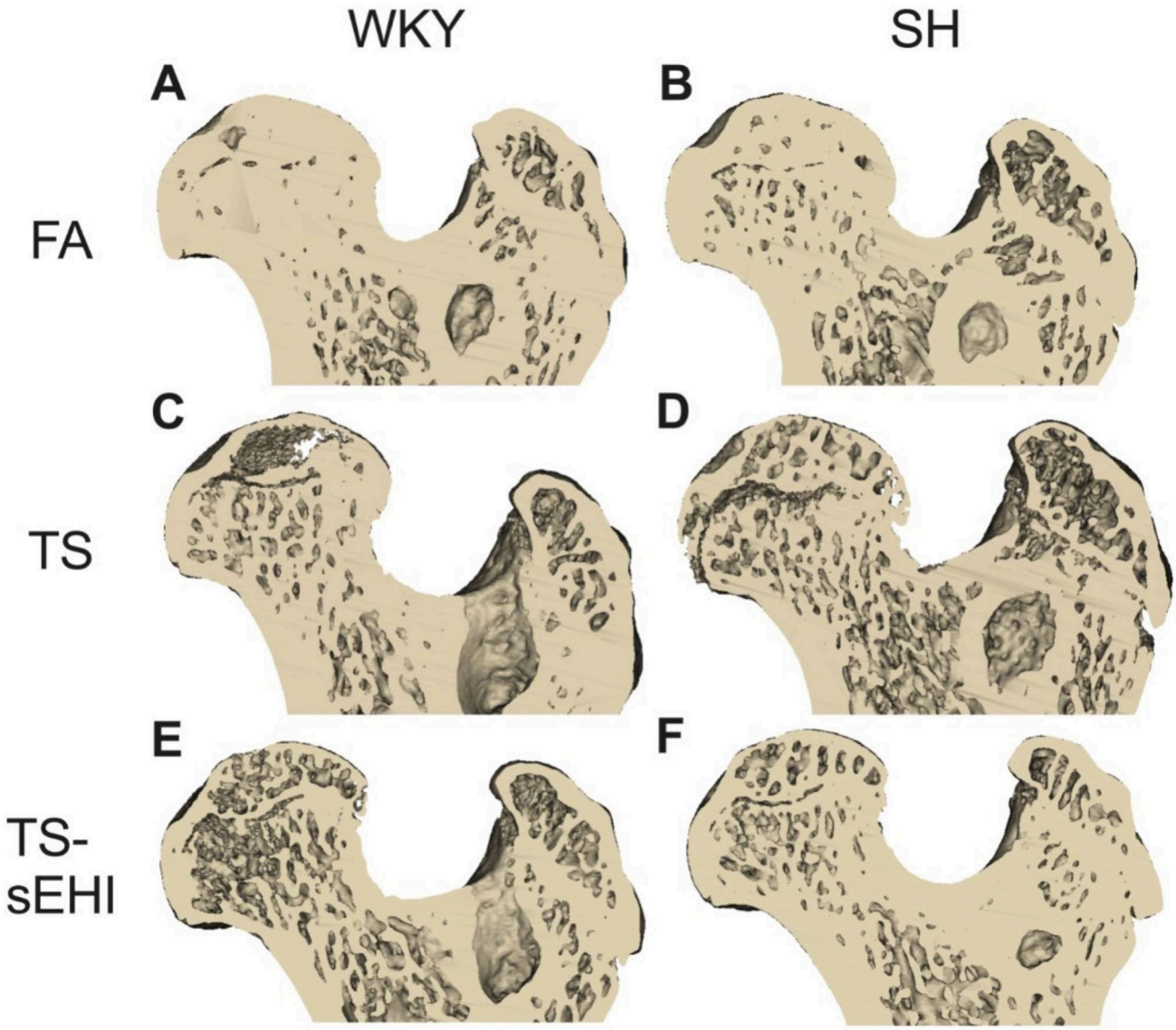

Fig. 4. Morphological influence of TS exposure and sEHI treatment on the femoral heads.

Representative coronal plane micro-CT-derived reconstructed 3D structure of the femoral heads from WKY or SH rats subjected to FA, TS, or TS plus sEHI. N = 6 per group. WKY, normotensive Wistar Kyoto rats; SH, spontaneously hypertensive rats; FA, exposure to filtered air; TS, exposure to tobacco smoke; sEHI, treatment with soluble epoxide hydrolase inhibitor.

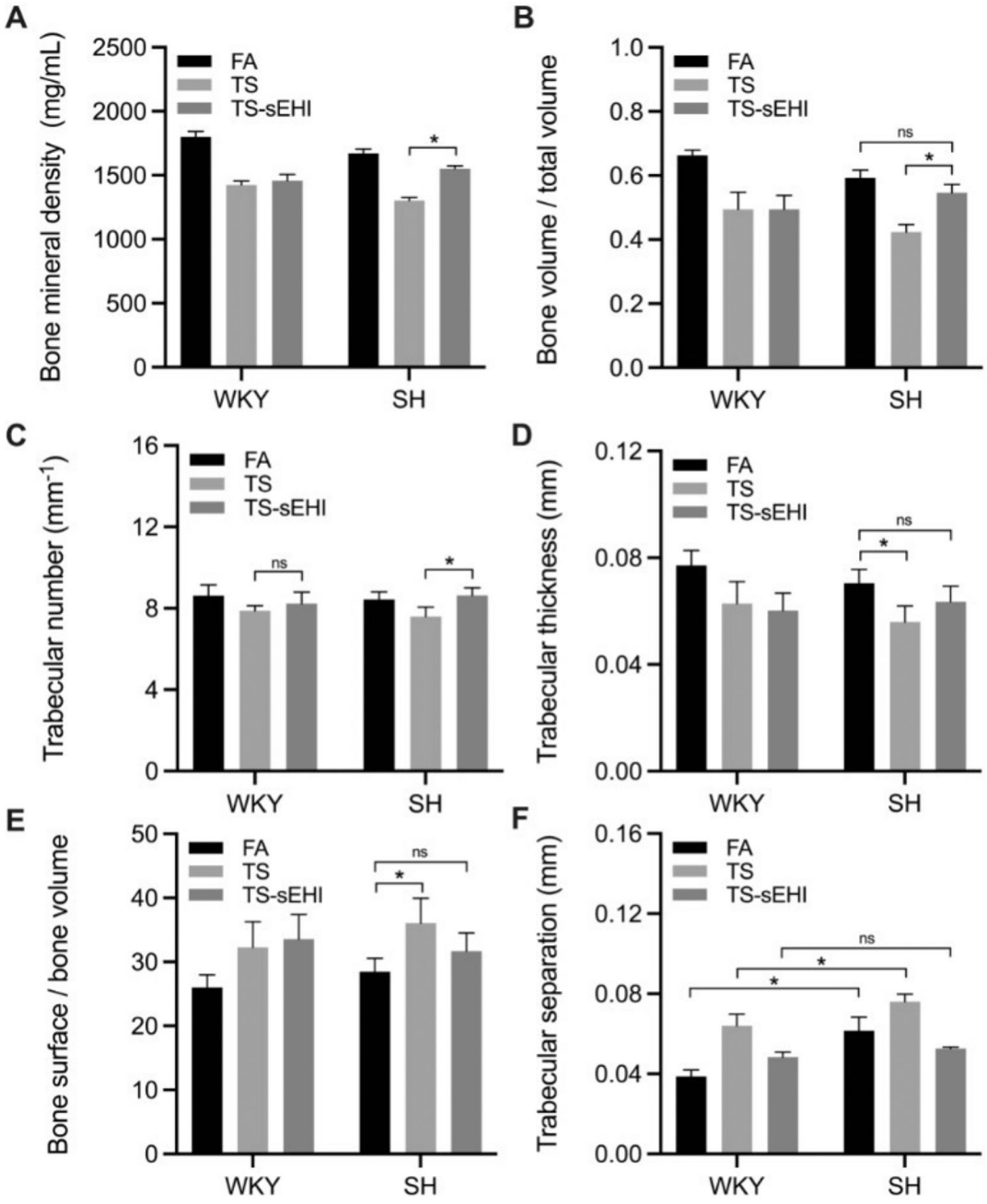

Fig. 5. Influence of TS exposure and eEHI treatment on the trabecular bone microarchitecture.

Micro-CT-derived trabecular bone morphometric indices including bone mineral density (**A**), bone volume/total volume (**B**), trabecular number (**C**), trabecular thickness (**D**), bone surface/bone volume (**E**), and trabecular separation (**F**) were obtained from the femoral heads of WKY or SH rats subjected to FA, TS, or TS plus sEHI. * $P < 0.05$ vs. the group indicated, ns = not significant, n = 6 per group. WKY, normotensive Wistar Kyoto rats; SH, spontaneously hypertensive rats; FA, exposure to filtered air; TS, exposure to tobacco smoke; sEHI, treatment with soluble epoxide hydrolase inhibitor.

Table 1.

Conditions for tobacco exposure

	Relative Humidity (% RH)	Temp (°C)	Carbon Monoxide (ppm)	Nicotine (mg/m^3)	Gravimetric TSP (mg/m^3)
Mean	37.53	77.87	240.55	9.04	61.79
±SD	±9.19	±1.1	±41.33	±3.71	±12.03

Note: TSP, Total Suspended Particulates.

Table 2.

Percent ossification stages of the femoral heads (%)

Rat strain	Treatments	Stage 0 No ossification	Stage 1 Less than ½ ossification	Stage 2 More than ½ ossification	Stage 3 Complete ossification
	FA	0	0	50	50
WKY	TS	17	17	17	50
	TS + sEHI	0	50	17	33
	FA	0	17	17	67
SH	TS	33	33	33	0
	TS + sEHI	0	33	33	33

Notes: WKY, normotensive Wistar Kyoto rats; SH, spontaneously hypertensive rats; FA, exposure to filtered air; TS, exposure to tobacco smoke; sEHI, treatment with soluble epoxide hydrolase inhibitor. N = 6 per group.

Table 3.

Percent osteonecrosis stages of the femoral heads (%)

Rat strain	Treatments	Stage 0 No osteonecrosis	Stage 1 ¼ to ½ osteonecrosis	Stage 2 ½ to ¾ osteonecrosis	Stage 3 More than ¾ osteonecrosis
	FA	83	17	0	0
WKY	TS	67	0	17	17
	TS + sEHI	100	0	0	0
	FA	67	33	0	0
SH	TS	50	17	17	17
	TS + sEHI	83	17	0	0

Notes: WKY, normotensive Wistar Kyoto rats; SH, spontaneously hypertensive rats; FA, exposure to filtered air; TS, exposure to tobacco smoke; sEHI, treatment with soluble epoxide hydrolase inhibitor. N = 6 per group.